



Manufacturing Engineering Society International Conference 2017, MESIC 2017, 28-30 June 2017, Vigo (Pontevedra), Spain

## Spacing roughness parameters analysis on the EDM of TiB<sub>2</sub>

A. Torres, C.J. Luis\*, I. Puertas

*Mechanical, Energetics and Materials Engineering Department, Public University of Navarre, Campus de Arrosadía, s/n, Pamplona 31006, Spain*

---

### Abstract

Titanium diboride (TiB<sub>2</sub>) is a novel sintered ceramic material which has attracted a great deal of interest because of its excellent mechanical properties, wear resistance and chemical resistance. At present, this ceramic is used in specialized applications in such areas as impact resistant armor, cutting tools, crucibles and wear resistant coatings. In this present research work, effects of current intensity, pulse time and duty cycle on the spacing roughness parameters Sm and Pc have been studied. In addition, statistical tools based on the design of experiments as well as multiple linear regression techniques have been used. Experimental results suggest that the optimal conditions to obtain a minimum Sm of 52.60 μm and a maximum Pc of 190.60 cm<sup>-1</sup> were: 2 A, 5 μs and 0.4, respectively, for current intensity, pulse time and duty cycle.

© 2017 The Authors. Published by Elsevier B.V.

Peer-review under responsibility of the scientific committee of the Manufacturing Engineering Society International Conference 2017.

*Keywords:* Roughness; EDM; TiB<sub>2</sub>; Manufacturing.

---

### 1. Introduction

Titanium diboride (TiB<sub>2</sub>) is a sintered ceramic material which has attracted a great deal of interest because of its excellent mechanical properties, wear resistance and chemical resistance [1]. In addition, unlike most ceramics, TiB<sub>2</sub> can be machined by electrical discharge machining (EDM) due to its good thermal and electrical conductivity [2]. At present, this ceramic is used in specialized applications in such areas as impact resistant armor, cutting tools,

---

\* Corresponding author. Tel.: +34-948-169301; fax: +34-948-169099.

*E-mail address:* [cluis.perez@unavarra.es](mailto:cluis.perez@unavarra.es)

crucibles and wear resistant coatings [3]. In addition, literature reveals that ceramics such as  $TiB_2$  and  $B_4C$  and some composites containing nitrides, carbides and borides can be shaped to an ultra-smooth finish [4].

Up to now, not many researchers have studied the machining of such ceramic, so the EDM of  $TiB_2$  is still a field to be investigated. In this line, Malek et al. [5] made an attempt to assess the interrelationships between microstructure, mechanical properties and EDM behavior of  $B_4C$ - $TiB_2$  composites with respectively 30, 40 and 60 vol.%  $TiB_2$ . Gaikwad and Jatti [6] tried to optimize EDM process parameter for maximization of material removal rate during machining of NiTi alloy. Rengasamy and Rajkumar [7] used  $TiB_2$  particles to reinforce Aluminum 4032 in order to analyse the influence of both mechanical properties and parameters such as material removal rate and tool wear rate in EDM process.

In this present study, an analysis of surface roughness of an EDM'ed  $TiB_2$  ceramic has been carried out. Concretely, the parameters selected were:  $S_m$  (mean spacing of profile irregularities) and  $P_c$  (peak count) which can be found in UNE-EN ISO 4287:1999 [8] and UNE-EN ISO 4287:1999/A1: 2010 [9]. Moreover, both parameters have been studied in terms of current intensity supplied by the generator ( $I$ ), pulse time ( $t_p$ ) and duty cycle ( $\eta$ ). To do that, statistical tools based on the Design Of Experiments (DOE) as well as multiple linear regression techniques have been used. Moreover, the adequacy of the proposed model has been carried out though analysis of variance.

## 2. Methodology and experimental procedure

In this section the equipment and the materials used to conduct the experimentation are first described. Then, the design of the experimentation is developed.

In the present study, the equipment used to conduct the experiments was a conventional die-sinking EDM machine model ONA DATIC D-2030 S. As a dielectric fluid, mineral oil was chosen as it improves the stability of the EDM process. The part and electrode materials selected were  $TiB_2$  and electrolytic copper, respectively. All the experiments were subjected to positive polarity as it was experimentally proved that a more stable process was obtained.

Once the experiments were carried out, surface roughness parameters were measured with a profile rugosimeter as can be seen in Fig. 1. The values of the cut-off and the evaluation length were 0.8 mm and 4 mm, respectively. Moreover, a Gaussian filter was used.

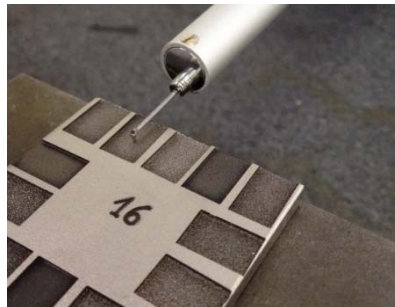


Fig. 1. Measurement of surface roughness.

Also, a factorial design  $2^3$  with four central points was selected. For the second-order model, six additional star points were used. Table 1 shows the design matrix for the second-order model and the results obtained in the experimentation.

Table 1. Design matrix and experimental values.

	I (A)	$t_i$ ( $\mu$ s)	$\eta$	Sm ( $\mu$ m)	Pc ( $\text{cm}^{-1}$ )
$2^k$	2	5	0.4	52.60	190.60
	6	5	0.4	67.40	149.60
	2	45	0.4	64.00	157.00
	6	45	0.4	91.00	110.80
	2	5	0.6	55.80	179.80
	6	5	0.6	70.60	140.80
	2	45	0.6	58.40	171.40
	6	45	0.6	94.40	107.20
Star points	2	25	0.5	56.60	178.40
	6	25	0.5	81.00	124.60
	4	5	0.5	66.60	151.00
	4	45	0.5	83.60	120.00
	4	25	0.4	71.80	140.60
	4	25	0.6	80.20	125.00
Central points	4	25	0.5	85.60	117.80
	4	25	0.5	78.00	129.20
	4	25	0.5	83.60	119.80
	4	25	0.5	74.40	135.40

### 3. Results and discussion

In this section the spacing parameters Sm and Pc are analyzed. Moreover, the models that characterize the behavior of these parameters are obtained. In order to decide which model is most suitable for its analysis, a lack-of-fit test as well as the values obtained for the coefficient of multiple determination ( $R^2$ ) and the coefficient of adjusted multiple determination ( $R^2_{\text{adj}}$ ) are used. For this specific study, both variables have been analyzed using second-order models.

Table 2 and Table 3 depict analysis of variance tables for Sm and Pc, respectively. For the case of Sm, four of the effects influence this variable. These effects, in order of importance, are: current intensity, pulse time, the quadratic effect of current intensity and the interaction effect between current intensity and pulse time. Also, in the case of Pc, three effects are statistically significant. These effects are: current intensity, pulse time and the quadratic effect of current intensity.

Table 2. Analysis of variance of Sm.

Source	Sum of Squares	Df	Mean Square	F-Ratio	P-Value
A: Current intensity	1368.90	1	1368.90	91.22	$5.87 \cdot 10^{-7}$
B: Pulse time	614.66	1	614.66	40.96	$3.40 \cdot 10^{-5}$
C: Duty cycle	15.88	1	15.88	1.06	0.3240
AA	343.79	1	343.79	22.91	0.0004
AB	139.45	1	139.45	9.29	0.0101
Total Error	180.07	12	15.01		
Total (corr.)	2662.74	17			

Table 3. Analysis of variance of Pc

Source	Sum of Squares	Df	Mean Square	F-Ratio	P-Value
A: Current intensity	5963.36	1	5963.36	123.59	$2.54 \cdot 10^{-7}$
B: Pulse time	2114.12	1	2114.12	43.82	$3.76 \cdot 10^{-5}$
C: Duty cycle	59.54	1	59.54	1.23	0.2903
AA	1991.86	1	1991.86	41.28	$4.90 \cdot 10^{-5}$
AB	115.52	1	115.52	2.39	0.1501
BC	115.52	1	115.52	2.39	0.1501
Total error	530.76	11	48.25		
Total (corr.)	10890.70	17			

Surface roughness results shown in Table 2 and Table 3 are plotted in Fig. 2 and Fig. 3 which represent the Pareto charts for Sm and Pc, respectively. From these figures, it can be observed that the most influential design factors on Sm and Pc turn out to be current intensity and pulse time. In addition, it can also be seen that both parameters exhibit opposite behaviors. That is, Sm tends to increase when current intensity and pulse time increase, whereas Pc decreases. A priori, this is the expected result since at high energy conditions, high rates of part material are removed resulting in a smaller number of craters (low Pc) but of larger diameter (high Sm).

This fact is observed in the experiment whose values of Sm ( $52.60 \mu\text{m}$ ) and Pc ( $190.60 \text{ cm}^{-1}$ ) are the lowest and the highest, respectively. In this case, both the current intensity (2 A) and the pulse time ( $5 \mu\text{s}$ ) are the minimum values within the selected range. By increasing both factors up to 6 A and  $45 \mu\text{s}$ , Sm increases significantly while Pc decreases, as observed in experiment whose values of Sm and Pc are  $94.40 \mu\text{m}$  and  $107.20 \text{ cm}^{-1}$ , respectively.

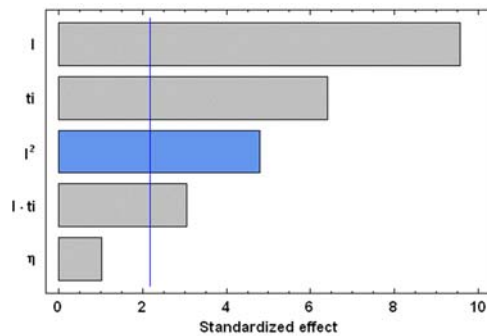


Fig. 2. Pareto chart for Sm.

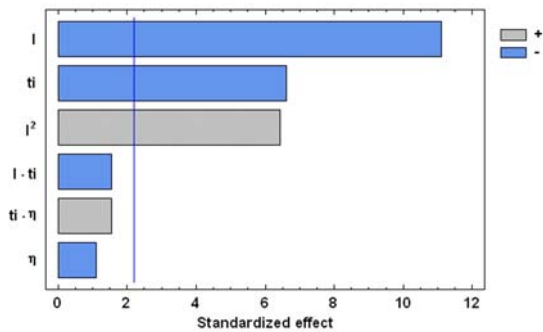


Fig. 3. Pareto chart for Pc.

In the case of Sm,  $R^2$  and  $R^2_{\text{adj}}$  values are 93.24 % and 90.42 % while for Pc the values of  $R^2$  and  $R^2_{\text{adj}}$  are 95.13 % and 92.47 %. These results indicate that the regression model is good enough to characterize the relationship between the factors selected and the spacing parameters. The equations of the adjusted model for Sm and Pc are given in Eq. (1) and Eq. (2), respectively.

$$Sm = 13.7325 + 20.8306 * I - 0.0255 * t_i + 12.6000 * \eta - 2.1988 * I^2 + 0.1044 * I * t_i \quad (1)$$

$$Pc = 307.9950 - 52.1750 * I - 1.2970 * t_i - 71.9000 * \eta + 5.2925 * I^2 - 0.0950 * I * t_i + 1.9000 * t_i * \eta \quad (2)$$

Additionally, Fig. 4 depicts surface roughness profile corresponding to experiment with the lowest Sm ( $52.60 \mu\text{m}$ ) and the highest Pc ( $190.60 \text{ cm}^{-1}$ ) values. As can be observed, profile is characterized by numerous peaks

that are very close to each other. On the contrary, spacing profile of Fig. 5 results larger and the peak count is considerably lower. In this case,  $S_m$  and  $P_c$  values are  $94.40 \mu\text{m}$ ,  $P_c = 107.20 \text{ cm}^{-1}$ , respectively.

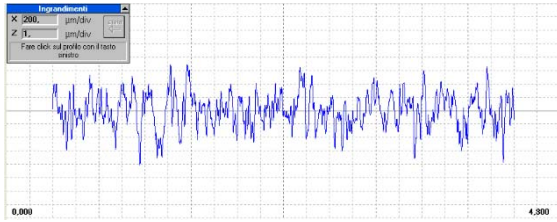


Fig. 4. Surface roughness profile of E1 (minimum  $S_m$  and maximum  $P_c$ ).

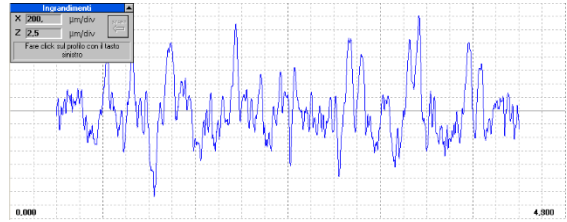


Fig. 5. Surface roughness profile of E8 (maximum  $S_m$  and minimum  $P_c$ ).

Fig. 6 illustrates the estimated response surface of  $S_m$  versus current intensity and pulse time. As can be observed, at high values of pulse time, there is a tendency for  $S_m$  to increase as the current intensity increases. This increase tends to diminish with current intensity values higher than 4 A due to the interaction effect between current intensity and pulse time. With respect to  $P_c$ , as depicts Fig. 7, the maximum values of  $P_c$  are obtained at low values of both current intensity (2 A) and pulse time (5  $\mu\text{s}$ ).

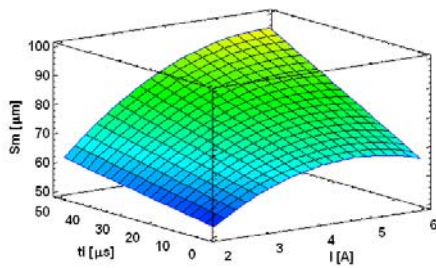


Fig. 6. Estimated response surface of  $S_m$ .

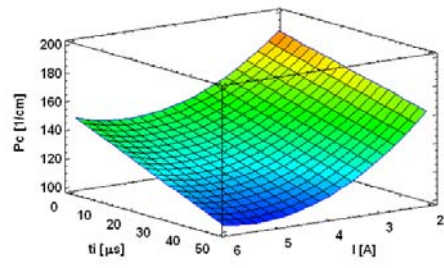


Fig. 7. Estimated response surface of  $P_c$ .

#### 4. Conclusions

For the case of  $S_m$  and  $P_c$ , both current intensity and pulse time are found to be the most significant factors, whereas duty cycle is not an influential factor. However, both parameters exhibit opposite behaviors: at high values of pulse time  $S_m$  tends to increase when current intensity increases, while  $P_c$  decreases. According to this, for the materials and work intervals selected in this study, low values of current intensity and pulse time should be selected in order to obtain low  $S_m$  values and high  $P_c$  values, which leads to a good surface finish.

Moreover, the optimal conditions to obtain a minimum  $S_m$  value of  $52.60 \mu\text{m}$  and a maximum  $P_c$  value of  $190.60 \text{ cm}^{-1}$  are: 2 A, 5  $\mu\text{s}$  and 0.4, respectively, for current intensity, pulse time and duty cycle.

#### References

- [1] S.H. Kang, D.J. Kim, J. Eur. Ceram. Soc. 27 (2007) 715-718.
- [2] S. Chao, J. Goldsmith, D. Banerjee, Int. J. Refract. Met. H. 49 (2015) 314-319.
- [3] R.G. Munro, Res. Natl. Inst. Stan 105 (2000) 709-720.
- [4] S. Lopez-Esteban, C.F. Gutierrez-Gonzalez, G. Mata-Osoro, C. Pecharroamn, L.A. Diaz, R. Torrecillas, J.S. Moya, Scripta Mater. 63 (2010) 219-222.
- [5] O. Malek, J. Vleugels, K. Vanmeelen, S. Huang, J. Liu, S. Van der Berghe, A. Datye, K.H. Wu, B. Lauwers, J. Eur. Ceram. Soc. 31 (2011) 2023-2030.

- [6] V. Gaikwad, V.S. Jatti, J. King Saud University - Engineering Sciences, <http://dx.doi.org/10.1016/j.jksues.2016.04.003>.
- [7] N.V. Rengasamy, M. Rajkumar, J. Alloy. Compd. 662 (2016) 325-338.
- [8] UNE-EN ISO 4287:1999, Especificación geométrica de productos (GPS). Calidad superficial: Método del perfil. Términos, definiciones y parámetros del estado superficial. AENOR, Madrid 1999.
- [9] UNE-EN ISO 4287:1999/A1: 2010, Especificación geométrica de productos (GPS). Calidad superficial: Método del perfil. Términos, definiciones y parámetros del estado superficial. Modificación 1: Número de picos. AENOR, Madrid 2010.